East European Journal of Physics. **1.** 31-42 (2024)
DOI:10.26565/2312-4334-2024-1-02 ISSN 2312-4334

THERMALLY ACTIVATED DELAYED FLUORESCENCE IN ORGANIC SEMICONDUCTORS AND ITS APPLICATION IN LIGHT EMITTING DIODES

Serhii Melnykov, Igor Helzhynskyy, Tetiana Bulavinets, Pavlo Stakhira
National University "Lviv Polytechnic", Department of Electronic Engineering, 1 St. Yura sq., Lviv, Ukraine
Corresponding Author e-mail: serhii.o.melnykov@lpnu.ua
Received October 31, 2023; revised December 26, 2023; accepted December 30, 2023

The presence of the effect of thermally activated delayed fluorescence (TADF) in organic light-emitting materials (emitters), manifested in the "collecting" of triplet excitons in organic semiconductor complexes that do not contain noble metals, creates excellent prerequisites for the application of TADF materials in the technology of manufacturing organic light-emitting diodes (OLED). The significant progress in solving theoretical and technical problems, achieved in the process of development of highly efficient TADF materials, paves the way for the formation of the future of organic electronics. This review presents the analyses of the nature of the long-term fluorescence generation mechanism at the molecular level and the up-to-date strategies for designing TADF donor-acceptor materials, as well as exciplex intermolecular complexes. Special attention is focused on the analysis of TADF emitter ambipolar materials with a highly twisted, rigid molecular structure, which reveal a tendency towards the multi-channel emission mechanisms and their implementation in a variety of OLED structure architectures.
Key words: *Organic light-emitting diodes; Thermally activated delayed fluorescence; Emitter; Multilayer structure; Exciton; Singlet-triplet energy splitting*
PACS: 78.55.Kz

INTRODUCTION

The current state of the OLED technologies development largely determines the commercial attractiveness of lighting systems based on organic LEDs and OLED displays, which have a number of advantages over the liquid crystal displays. In particular, the OLED displays are thinner and weigh less. In addition, they are characterized by a wide viewing angle (up to 180^0) and higher color contrast. A significant argument that opens up new design possibilities for the production of OLED displays and their implementation on the electronic equipment market is the technological capability of forming OLED displays on flexible substrates with the functional possibility to bend and unfold the screen. Regarding the expediency of using organic LEDs in light-emitting devices, here, first of all, the low energy consumption of OLEDs and the absence of toxic substances in their design should be noted, which creates prerequisites for both global energy saving and reducing the industrial burden on the environment [1].

The organic light-emitting diodes (OLED**s**) are electroluminescent devices with a multilayer structure of organic semiconductor materials sandwiched between a transparent anode and a metal cathode (Fig. 1). When an external voltage is applied to the OLED electrodes (cathode and anode), the charge carriers (electrons and holes) enter the electron and hole injection layers, respectively, with further injection into the electron and hole transport films, from where they drift into the emissive (light-emitting) layer in which, under the influence of the Coulomb interactions form excitons [2-4].

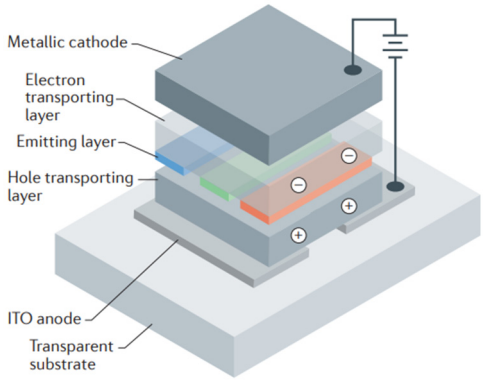

Figure 1. Schematic representation of the multilayer structure of the device based on an organic light-emitting diode (OLED)

Inherently, the excitons represent an emitter molecule in an excited state (Fig. 2). The molecular excited states can be classified as electrically balanced states formed by the exchange of energy and charge between neighboring molecules of singlet or triplet character. In the emitter molecule, there exist simultaneously two systems of electronic levels: singlet S_n and triplet T_n.

Cite as: S. Melnykov, I. Helzhynskyi, T. Bulavynets, P. Stakhira, East Eur. J. Phys. 1, 31 (2024), https://doi.org/10.26565/2312-4334-2024-1-02

The triplet excitons have a rather long lifetime, since the radiative transition to the ground state is forbidden. This is equivalent to the indirect transitions in crystals. The triplet excitons can diffuse over long distances (up to 100 nm), while the singlet ones cannot diffuse more than 10 nm.

A definite set of vibrational states corresponds to each energy level. Both radiative and non-radiative transitions can occur during the transition of an excited molecule to an equilibrium state. In this context, internal conversion (IC) and Intersystem crossing (ISC) are distinguished. The internal conversion is characterized by intramolecular transitions between different electronic states of the same multiplicity, for example, $S_2 \rightarrow S_1$ (singlet-singlet) and $T_2 \rightarrow T_1$ (triplet-triplet). It should be noted that the probability of such transitions is the greater, the smaller is the difference between the energy levels of the initial and final state.

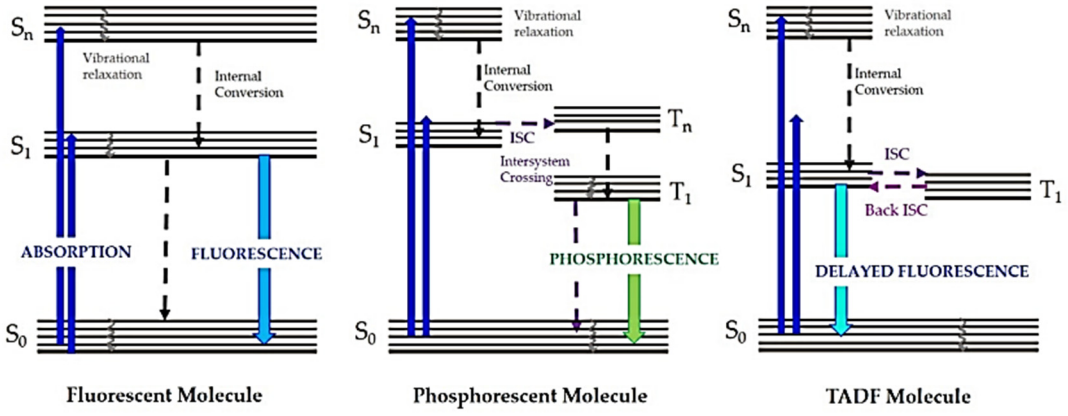

Figure 2. Energy level diagram that shows the main luminescence processes in an emitter molecule (left: fluorescent molecule; center: phosphorescent molecule; right: TADF molecule). Continuous arrows indicate radiative processes. Dotted arrows represent non-radiative relaxation

The total electron spin for the singlet state is zero, because the electrons are paired. For the triplet state, the total spin is equal to two, and the multiplicity, as opposed to one, for the singlet state corresponds to three, respectively. Generally, the basic unexcited state (state S_0) of organic molecules is singlet, and therefore, theoretically, a radiative transition from the lower singlet excited state - S_1 to the basic S_0 state is allowed. Such a radiative transition with short relaxation time in the nanosecond range is called fluorescence.

Unlike the phosphorescence, which is a theoretically forbidden radiative transition of triplet excitons from the lower triplet excited state T_1 to the main S_0, the recombination time is in the microsecond or millisecond range. Note, that the relaxation time for triplet transitions is significantly reduced under the influence of such external factors, as heat or oxygen, on the emitter molecule [5, 6]. The intercombination conversion, that is, transitions between two isoenergetic vibrational levels, refers to the states of different multiplicity. For example, a molecule from the zero vibrational level of the S_1 state can move to the isoenergetic vibrational level of the triplet state T_2, and then, as a result of vibrational relaxation, to the T_1 level. The transitions between the states of different multiplicities are, in principle, forbidden, however, the spin-orbit overlap may be sufficient to partially remove the prohibition [7-9].

It should be noted, that the presence of rare-earth metals (eg, Ir and Pt) increases the probability of spin-orbit overlap and, thus, increases the probability of intercombination conversion resulting in phosphorescence at the room temperature. Thus, this approach makes it possible to involve both triplet and singlet excitons in the process of light recombination, which theoretically allows obtaining a value of the external quantum efficiency (EQE) of the device close to 100%. Today, the maximum EQE value of the organic phosphorescent OLEDs, based on the latest phosphorescent metal complexes, shows a very high value, more than 50% [10-13].

SINGLET-TRIPLET ENERGY SPLITTING (ΔE_{ST}) AND TADF MECHANISM

The TADF-based organic LEDs use molecular systems with a small energy split between singlet and triplet states. This can be realized either in intramolecular charge transfer states of molecules with nearly orthogonal donor and acceptor parts, or in intermolecular exciplex states formed between an appropriate combination of individual donor and acceptor materials. These processes are described in more detail in our previous works [14-165,6,7]. Another method of using triplet excitons in OLEDs is the use of emitters that exhibit thermally activated delayed fluorescence. In fact, this type of molecule has a narrow energy gap between the triplet and singlet excited states, so that the thermal energy, inherent at the room temperature, is sufficient to activate the reverse Intersystem crossing (ISC (reverse ISC)), promoting the complete conversion of the triplet state to the singlet one, thus triggering the collection of singlets. When the gap is close to zero, the reverse intersystem crossing (RISC) is possible [17-19]. The most promising and effective approach to the collection of triplet excitons involving the RISC process is the use of TADF emitters. In the RISC TADF emitter, the thermal motion of the molecule at sufficiently high temperatures (more than 300 K) can easily activate the conversion. The efficiency of TADF is mainly determined by the temperature sensitive RISC process. The functional dependence of the RISC rate constant (k_{RISC}) on the temperature can be expressed by the Boltzmann equation:

$$k_{RISC} \propto \exp(\Delta E_{ST}/k_B T) \quad (1)$$

where T is the temperature and k_B is the Boltzmann constant.

It is well known that the presence of a narrow energy gap ΔE_{ST} of less than 0.2 eV in the emitter molecules enables an effective RISC process [20]. ΔE_{ST} can be defined as the energy difference of the lowest singlet (E_S) and triplet (E_T) excited states:

$$E_S = E + K + J, \quad (2)$$

$$E_T = E + K - J, \quad (3)$$

$$\Delta E_{ST} = E_S - E_T = 2J, \quad (4)$$

where E is the orbital energy, K is the electron repulsion energy, J is the exchange energy or the exchange integral [21].

$$J = \int_{\infty}^{o} F_D(\lambda)\epsilon_A(\lambda)\lambda^4 d\lambda, \quad (5)$$

where $F_D(\lambda)$ is the normalized emission spectrum of the donor, ϵ_A is the standard for the molar absorption coefficient of the acceptor, and λ is the wavelength.

We remind that as a result of a conjugated bond formation in organic semiconductors, bonding π- and excited π^* molecular orbitals are formed. These orbitals form narrow energy levels that split into zones. The filled π -orbital is called the highest occupied molecular orbital (HOMO), and the excited π^*-orbital is called the lowest vacant molecular orbital LUMO (lowest unoccupied molecular orbital).

Thus, the value of the energy gap ΔE_{ST} is two times greater than that of J. Equation (4) shows that a small value of ΔE_{ST} can be obtained using a small overlap integral (5), i.e. by separating the HOMO and LUMO spatial wave functions. Note, that the molecular TADF emitters are the structures consisting of donor-acceptor (D-A) or donor-acceptor-donor (D-A-D) components, which are characterized by intramolecular charge transfer states between the acceptor and donor components. These emitter TADF components are so far apart in the orthogonal orbitals, that the spin-orbit interaction between them is very small, what makes the RISC scenario unlikely. From the molecular point of view, a spatially twisted structure can ensure a small value of ΔE_{ST}, since with an effective distribution of NOMO and LUMO, the value of the exchange integral can be small. A value of ΔE_{ST} close to zero can be obtained by spatial separation of the electron densities of the frontier orbitals, as shown in Fig. 3a. The spatial separation of the electron densities of NOMO and LUMO levels in the molecule with a twisted D-A structure is shown in Fig. 3 b. The right-angle rotation between the D and A components is important for the formation of the TADF molecule. These two key factors between the ^{1}CT singlet state and the ^{3}CT triplet state with a small energy gap provide TADF emission.

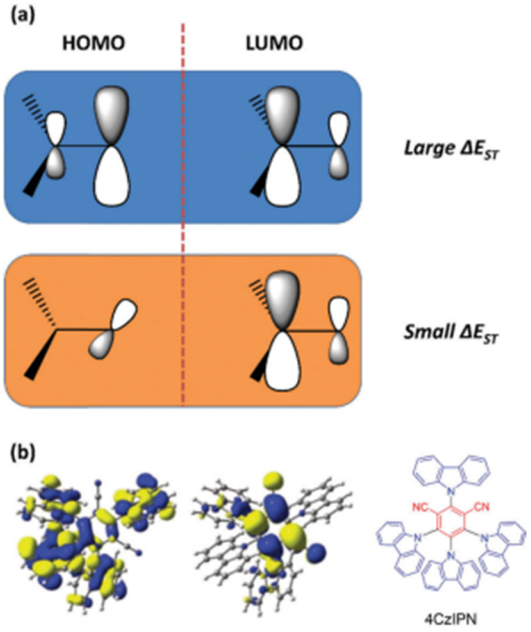

Figure 3. (a) Strategy for realizing small ΔE_{ST} values in the organic TADF molecules. HOMO: the highest occupied molecular orbital, LUMO: the lowest unoccupied molecular orbital, ΔE_{ST}: the energy gap between the S_1 and T_1 states. (b) Electron density in the HOMO and LUMO of the typical example (4CzIPN) of the organic TADF molecules with a twisted molecule of the D–A structure type. The inset shows the molecular structure. [22].

Besides the optimal values of ΔE_{ST} and k_{RISC}, a relatively large value of the radiation rate constant k_r, which is the rate of transition of a singlet exciton from the S_1 state to the S_0 one, is also important for obtaining effective TADF emission. However, the large value of k_r and close to zero ΔE_{ST} conflict with each other, what requires careful design of molecular structures for simultaneous implementation of the proper parameters. For example, some ketone derivatives

have a relatively small value of $_{\Delta}E_{ST}$, but exhibit phosphorescence only at low temperature due to the large value of k_r for the triplet excitons [23-25]. On the other hand, due to the special conjugation combination, resulting from the twisted central group –CQ= in several diphenyl-ketones with different donor groups attached to the phenolic ring, there is a specific double TADF emission of white colour. Unlike the typical fluorescent emitters with rather narrow emission spectra, the TADF emitters usually exhibit poorer monochromeness. To improve the purity emission, steric hindrances are introduced into the TADF emitter core or intensify the stiffness of the acceptor fragment and, thus, suppress the molecular rotation between the donor and acceptor components [22, 26]. Another key direction that allows overcoming the limitations on the use of fluorescent dyes in the electroluminescent devices' technology is the study of promising TADF emitters with the aggregation induced effect. The fact is that under the influence of the π - π interaction the TADF molecules are easily aggregated, what causes the aggregation-caused luminescence quenching (ACQ). This effect seriously limits the use of TADF emitters in optoelectronic devices. To overcome the occurrence of ACQ, numerous organic dyes with aggregation-induced emission (AIE) properties have been developed in the last decade. In fact, solutions of AIE luminophor are characterized by extremely low photoluminescence quantum efficiency, while their luminescence is sharply enhanced in the solid state. Such a phenomenon of enhanced emission is usually interpreted as a limitation of intermolecular rotations and the twisted Intramolecular Charge Transfer (TICT). Therefore, the charge transfer mechanisms and twisted molecular structures have a crucial effect on the photophysical properties of the TADF emitters, which are important for the high-performance OLED devices.

Besides the TADF exciplexes in this paper, i.e. the TADF emitter molecules with the AIE effect, attention is paid to highly twisted TADF molecules of the D-A type, subject to their molecular configurations. We also focus on developing the design and photophysical processes commonly used to optimize the TADF technology of the OLED device.

TADF EMITTERS BASED ON A DONOR-ACCEPTOR PAIR

Relative simplicity of the synthesis as well as the high quality of light emission of the TADF emitters, based on a donor-acceptor pair, determines their wide use in organic optoelectronic devices. However, the presence of a large twist angle between the D and A fragments can promote the significant steric hindrances. In this context, the use of ortho-D-A-compounds is a simple and effective strategy for the formation of an almost vertically twisted molecular configuration to obtain the smallest possible value of ΔE_{ST}, as well as an efficient TADF process. Su and colleagues [27] developed a series of D–A molecules based on TRZ groups acting as the acceptors and the dibenzothiophene or thianthrene (TE) derivatives as the donors. The presence of the influence of heavy sulfur atoms promoted an increase in the SOC coefficient and, as a result, enabled the passage of ISC. In the singlet state of oTE-DRZ (Fig. 4), the rigid molecular environment prevented the occurrence of a non-radiative transition, while the available permitted phosphorescent transitions promote further cascade conversion and the increase of the long-lived triplet excitons lifetime.

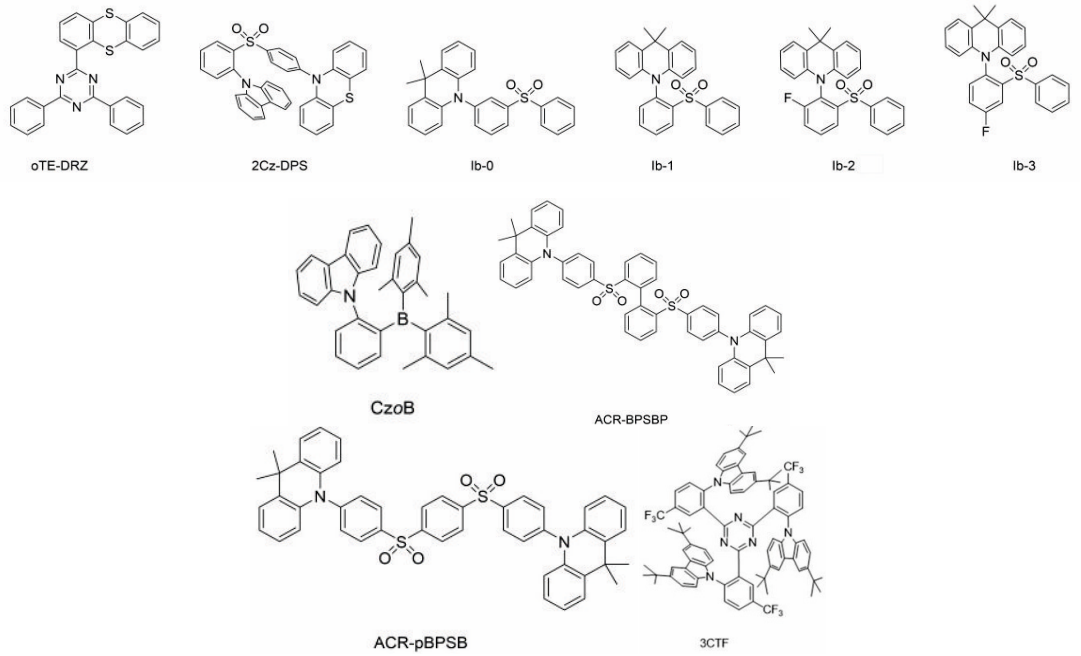

Figure 4. Molecular structure of TADF emitters based on a donor-acceptor pair.

It was found that the oTE-DRZ crystal (Fig. 4) exhibited the dual channel properties (TADF and the room temperature phosphor luminescence (RTP) with greenish-blue luminescence of photoluminescence quantum yield (PLQY 87%) (Fig. 5) due to the limitation of intermolecular and intramolecular degrees of motion freedom. Owing to the presence of strong π–π intermolecular bonds, the OLEDs based on o TE-DRZ thin films showed the EQE of up to 20.6%. To achieve a high IQE for the simple TADF emitters Chi and colleagues [28] reported about the development of a new

molecular design and the synthesis of twisted molecular TADF emitters by introducing an ortho-bonded carbazole donor link, which forms an asymmetric D–A–D' structure. The close spatial proximity of the donor and acceptor in the asymmetric structure can intensify through-space charge transfer (TSCT), thereby suppressing molecular vibrations, thus preventing the energy loss. The X-ray diffraction data indicate a substantial bond between phenothiazine (D') and diphenylsulfone (A). Due to the two-channel mechanism of the charge transfer (CT), the molecular compound 2Cz-DPS (Fig. 4(42)) shows a high value (91.9%) of solid-state PLQ and the maximum quantum yield of electroluminescence = 28.7%. The same team [29] developed and synthesized two twisted D-A molecules characterized by ultra-long RTP and TADF relaxation time, namely o-Cz and p-Cz, in which the carbazole donor and the benzophenone acceptor were involved as they were combined by ortho- and the pair-method. Such molecules have been shown to exhibit a small ΔE_{ST}, that contributes to ISC and RISC under the dual-channel CT conditions, which in turn increases the number of triplet excitons involved to increase the TADF efficiency. Ultimately, o-Cz demonstrated the ultralong lifetime of 0.84 s and the quantum efficiency of 16.6%. To balance the lifetime and the emitter PLQY, Wang and colleagues [30] designed and synthesized three TADF molecules with a twisted structure based on diphenylsulfone and 9,9-dimethyl acridine groups. By removing the phenyl group from lb-Ph to reduce the distance between the D and A fragments, the through-space charge transfer TSCT can be achieved. The materials were characterized by multifunctional emissive properties, including TADF, the room temperature phosphorescence, aggregation, and triboluminescence (TL), which can be induced by a mechanical irritant action. The molecules exhibiting TSCT were found to show the PLQY value of nearly 100%. lb-1 (Fig. 4 (44)) and lb-3 (Fig. 4(46)) show obvious TL properties (Fig. 5). The both crystals showed good crystal clarity after grinding, which indicated good mechanical stability of the materials.

Although the effective TADF blue emitter materials are necessary for the commercialization of organic light-emitting diodes, there are a number of unsolved problems when implementing them into the technological route of the OLED fabrication. In particular: the high frequency of their emission negatively affects the effective life of blue OLEDs due to the rapid degradation of the emitting material [31-33]. Besides, a typical problem for such devices is a rapid performance degradation in the mode of high brightness. Therefore, the development of stable blue emitters for OLEDs is one of the most difficult tasks. Kido and colleagues [34] proposed a new strategy to obtain the blue TADF using 9,9-dimethyl-9,10-dihydroacridine (ACR) groups as the donor and double sulfonyl groups as the acceptor. ACR-BPSBP (Fig. 4) and ACR-pBPSB (Fig. 4) molecules had the same donors and the acceptors, but were characterized by different bonds. Compared to the ACR-pBPSB (Fig. 4), the ACR-BPSBP molecule (Fig. 4) has a more twisted structure and exhibits a higher PLQY due to the limitation of the conjugation length. Since the ACRBPSBP material (Fig. 4) showed steric difficulties on the part of the ortho-phenylsulfonyl group, the orthogonal configuration with a large twist angle of 85° was chosen. This molecule exhibited blue emission with the emission maximum in the region of 460 nm and with PLQY = 82%. However, the elongated ACR-pBPSB (Fig. 4) exhibited green emission with the maximum of 490 nm and the PLQY of 76%.

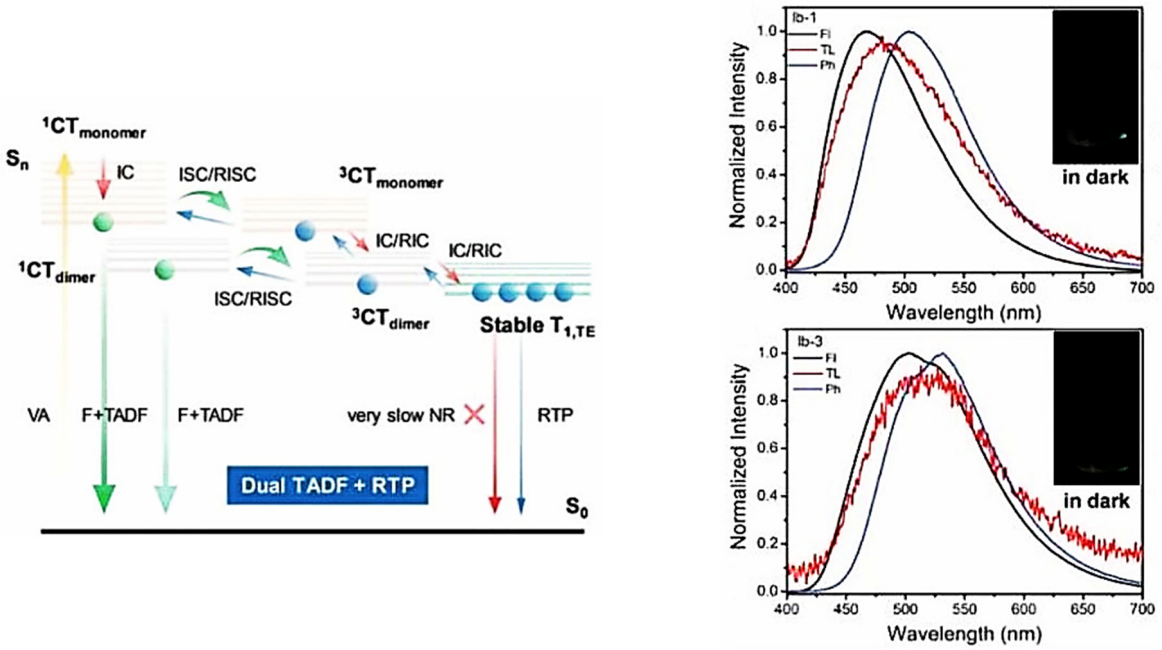

Figure 5. Diagram of the energy excited levels of ^{1}CTF, ^{2}CTF and ^{3}CTF (a). Fluorescence (Fl), triboluminescence (TL), and phosphorescence (Ph) spectra of lb-1 (44) and lb-3 (46) in the solid state (b)

ORGANIC LEDs BASED ON NON-DOPED TADF EMITTERS

The non-doped emitter layers in the OLED structure have a number of advantages as to the "doped" systems (guest-host): in particular, the manufacturing process is simplified, also most of the non-doped devices are characterized

by a lower supply voltage, higher brightness and a smaller drop in their efficiency than the doped devices. Besides, the inhomogeneities arising during the phase separation in the guest-host system, which are absent in the non-doped emitter, are harmful to the color stability and efficiency of the device. However, in terms of the quantity, the OLEDs based on the non-doped emitter layers are significantly inferior to the doped ones. The proper thermal and photochemical stability of TADF non-doped emitters is an important condition for their use in the OLED technology. Such a stability can be judged from the dissociation energy of the molecular bonds. The example of the presence of a relatively high bond dissociation energy, which promotes the increase in the effective life of TADF - OLED, is observed in the emitter molecule based on the combination of a stable acceptor (triazine) and a donor fragment (carbazole) [35-37]. Also, the key OLED parameter is the value of the external quantum efficiency (η_{EQE}), which can be represented as η_{EQE} =IQE×η_{out}, where IQE and η_{out} are the internal quantum efficiency of the device and the light output coefficient, respectively. For the TADF-based OLEDs, the formula for determining IQE is written down as:

$$\text{IQE} = \left[0.25\Phi p + \{0.75 + 0.25(1 - \Phi p)\}\frac{\Phi d}{1-\Phi p}\right]\gamma, \quad (6)$$

where γ is the charge balance coefficient, Φ_p and Φ_d are the contribution of instantaneous fluorescence and delayed fluorescence to the quantum yield of photoluminescence (Φ_{PL}) respectively: $\Phi_{PL}=\Phi_p + \Phi_d$. The γ value makes virtually 1.0 for most of modern multilayer OLEDs.

The non-doped OLEDs based on the green emitting molecule DMAC-BP show the EQE value and the maximum brightness of 18.9% and ~50,000 cdm^{-2}, respectively [38]. DBT-BZ-DMAC-based organic LEDs showing combined emission, which is caused by aggregation and TADF, have the maximum EQE of 14.2% and the slight drop in the current efficiency of 0.46% from the peak values to the values at 1000 cdm^{-2} [39]. Also, in a non-doped green OLED with the CP-BP-PXZ-based emitter, whose peculiarity is the presence of the long-term aggregation-induced fluorescence, showed the EQE value of 18.4% with a slight drop in the current efficiency of 1.2% at 1000 cdm^{-2} [40]. Exciplex TADF OLEDs are another type of the non-doped devices (Fig. 6.).

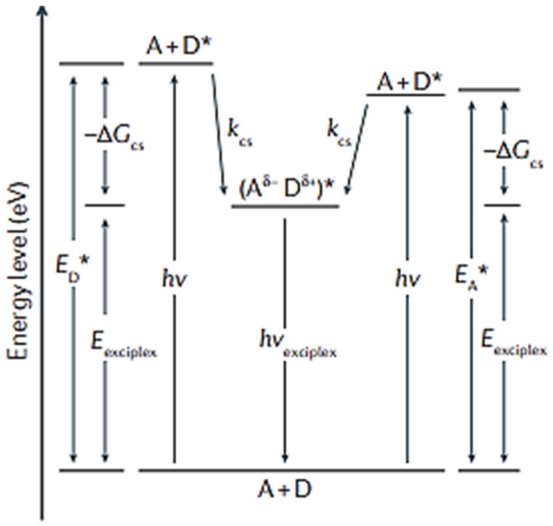

Figure 6. Electronic energy diagram demonstrating the process of exciplex formation and interconnection at the energy levels First, the donors and acceptors form the excited ground-state donors and acceptors or form the excited ground-state acceptors and donors upon the high-energy excitation. Then, the donor excitons and acceptor excitons combine into an exciplex. And finally, the exciplex splits into a donor and an acceptor component. In this case, a transition to the ground state with emission occures.

The exciplexes are the complexes in the excited state (CT), which are formed as a result of the interfacial interaction of an excited molecule (for example, an acceptor) with the other unexcited molecule (for example, a donor) (1A* + D → 1(A D)*). Then, the complex disintegrates into a positive hole and a negative electron with the transition to the S_o ground state with light emission. The electrostatic interaction of a positively charged donor with a negatively charged acceptor, which are located at a short distance from each other, enables exciplex stabilization. Similar to the intramolecular TADF in the TADF exciplex compounds, the spatial orientation of the HOMO and LUMO positions for D and A components and the intermolecular distance between them determine the formation of the RISC mechanism. It was found that the exciplexes, which emitted relatively high-energy light, were characterized by a relatively small CT energy from molecule to molecule and vice versa. Simulation of the emission energy in the solid phase showed the CT state to depend on the intermolecular distance between D and A molecules and their spatial orientation. To confirm this fact, the experimental observations were performed. An exciplex layer was formed with the 1:1 molar ratio of tris(4-carbazol-9-ylphenyl) amine (TCTA) and 4,6-bis(3,5-di(pyridin-4-yl)phenyl)-2-methylpyrimidine (B4Py -MPM) on the glass substrate [41]. The chemical structures and energy levels of TCTA and B4PyMPM are shown in Fig. 7 a. The positions of the HOMO level were determined by UV photoelectron spectroscopy, and the LUMO levels were calculated from the HOMO level and

the absorption edge of the UV absorption spectrum. The film absorption spectrum corresponds to the absorption spectra of TCTA and B4PyMPM, indicating that no aggregation or formation of the ST complex has occurred in the solid state. Fig. 7 b shows the spectral time dependence of the exciplex emission. The change in the time parameter of the intense light pulse was recorded by a high-speed photo-recording camera. The photoluminescent excitation of the samples was carried out using a pulsed nitrogen laser with the generation wavelength of 337 nm. The presence of different time spectral distributions indicates fast and slow mechanisms of the exciplex fluorescence decay. The integrated emission spectrum is dominated by exciplex emission. A gradual spectral shift into the low-energy area was observed, so, with the radiation shift from λ = 493 nm at the beginning of the area, a fast emission region (t = 0-10 ns) to λ = 535 nm, and in the long-wave area a slowed-down emitting band (t = 10−70 μs) was observed. The spectral red shift with the delayed emission is a feature of the exciplex caused by the effect of polarization under the influence of the host medium [42,43].

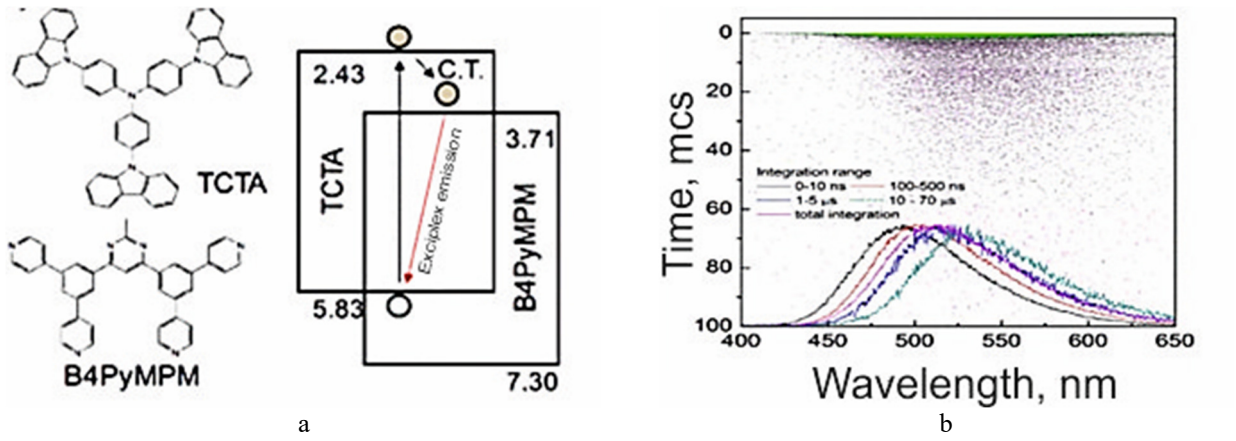

a b

Figure 7. a) Chemical structures of tris(4-carbazol-9-ylphenyl)-amine (TCTA) and 4,6-bis(3,5-di(pyridin-4-yl)phenyl)-2-methylpyrimidine (B4PyMPM) with the energy levels, b) time dependences of photoluminescence amplitude spectra of the exciplexes

To increase further the efficiency of using the exciplex approach in the technology of organic light-emitting devices, it is advisable to develop molecules with a high PLQY level for the use of D and A, while in order to minimize the quenching of triplet states in the TADF process, the donor and acceptor molecules should contain high-energy triplet energy levels [44, 45].

OLED BASED ON THE DOPED TADF EMITTER

To prevent the excitons annihilation in the organic LEDs, based on the doped TADF systems (guest-host), the emitter is usually dispersed into a solid-state matrix film (into the host component). A number of requirements are imposed on the host material, in particular: the triplet energy of the matrix molecule must be higher than that of the TADF emitter, the HOMO and LUMO levels must be correctly oriented, the organic matrix semiconductor must be characterized by a wide band gap and bipolar mobility of the charge carriers to maximize the formation of excitons in the emitter layer. Besides, the matrix should be morphologically stable and have good film-forming properties. In most cases, in the production of organic LEDs with TADF emitters traditional starting materials were used, which had been originally developed for the phosphorescent metal-organic complexes based on heavy metals [46]. The typical matrix molecules with high triplet energies are: DPEPO (T1: 3.3 eV) [47], PPF (T1: 3.1 eV) [48], mCPCN(T1: 3.03 eV) [49], CzSi (T1 3.0 eV) [49], mCBP (T1: 2.9 eV) [50], TPBi (T1: 2.7 eV) [51]. For the highly efficient green emitter 4CzIPN, several materials with the host function were synthesized [52-54], with which the quantum efficiency of up to 31.2% was observed for OLEDs (Table 1). Many matrix materials have been developed for the DMAC-DPS blue emitter. In particular, the OLED with the maximum EQE of 23.0% was obtained using DPE**T**PO as the host component [55]. It should be noted that due to the local dipole interaction, the polar matrix films can stabilize the CT excited state of the guest emitter. In this case, the emission of TADF OLED shifts to the red region of the spectrum. Thus, for the blue TADF-emitter DDMA-TXO2 due to combining the emitter with the matrix of the correct polarity, the energy of the ^{1}CT state decreases, and ΔE_{ST} is minimized, as a result of which EQE reaches the values of 22.4% for the device with CIE coordinates (0.16, 0 ,24) [56].

Table 1. Photoluminescence and electroluminescence characteristics of representative low-molecular TADF materials

Molecule		**Λ_{PL} (nm)**	**ΔE_{ST} (eV)**	**Φ_{PL} Host/ toluene (%)**	**τ_{PF} (ns)/ τ_{DF} (μs)**	**CE (cdA^{-1})**	**PE (lmW^{-1})**	**EQE_{max} (%)**
DMAC-DPS	PL:mCP film (10wt%)	464	0.09	90/80	2.1/3.1	-	-	19.5
	EL:DPEPO film (10wt%)							
	mCP film (10wt%)					-	19	19.5
	PL:mCP film (10wt%)					39.7	44.4	23.0
	EL:DPEPO film (10wt%)							

Molecule		Λ_{PL} (nm)	ΔE_{ST} (eV)	Φ_{PL} Host/ toluene (%)	τ_{PF} (ns)/ τ_{DF} (μs)	CE (cdA^{-1})	PE (lmW^{-1})	EQE_{max} (%)
DMAC-TRZ	mCPCN film (8wt%)	495	0.05	90/83	20.3/1.9	66.8	65.6	26.5
	PL: mCPCN film (10wt%) EL: neat film					61.1	45.7	20
4CzIPN	CBP film (6wt%)	507	0.08	93.8/-	17.8/5.1	-	-	19.3
	3CzPFP (1%)					-	-	31.2
PXZ-TRZ	CBP film (6wt%)	545	0.08	66/43	20/1.1	-	-	12.5
DACT-II	CBP film (9wt%)	529	0.009	63.7/100	-/-	-	-	29.6
TPA-DCPP	Neat film	708	0.13	14/84	20.8/0.76	4.0	-	9.8
HAP-3TPA	26mCPy film (6±1wt%)	610	0.17	91/-	-/100	25.9	22.1	17.5

White TADF OLEDs have found wide application in the up-to-date display devices and lighting systems, what created the prerequisites for further investment in their research area. White TADF OLEDs are usually obtained by mixing the three primary red, green, blue (RGB) emitting colors, for example: green (4CzPN), red (4CzTPN-Ph) and blue (3CzTRZ) emitters from the matrix (mCBP and PPT) [57-59]. With the optimized hetero structure consisting of 4CzPN: mCBP(3 nm)/4CzTPN-Ph:mCBP (2 nm)/3CzTRZ:PPT (10 nm), the TADF OLED device achieved the maximum EQE value of 17.6% and CIEx, y (0.26, 0.38). The aplication of hybrid "warm-white" WOLEDs, obtained using the TADF emitter of blue color (2CzPN) and yellow phosphor PO-01 in separate emitting layers (Fig. 8), made it possible to achieve the EQE_{max} values of 22.6% and (CIEx, y = (0.45, 0.48)) [34]. By combining the yellow TADF emitter PXZDSO2 with the dark blue fluorescent emitter NI-1-PhTPA, the warm white LEDs were fabricated achieving the EQE_{max} of 15.8% (CIEx,y = (0.401, 0.476). Furthermore, when the dark-red fluorescent component was inserted, the three-color white OLEDs were obtained with EQE_{max} = 19.2% (CIEx,y=(0.348, 0.577)), with a very high color rendering index of 95 [59,60].

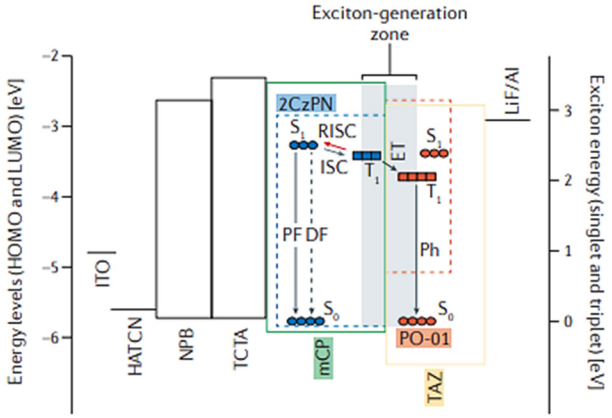

Figure 8. Energy levels, exciton energies and light emission mechanism of materials used in the hybrid white organic LEDs. The hybrid white OLED has two emissive layers (EML). The first EML, close to the hole transport layer (NPB), contains 2CzPN in the mCP matrix. In the second EML, located next to the electron transport layer, PO-01 is doped into the matrix. The emissive layers are located between the TAZ electron transport layer and the TCTA electron/exciton blocking layer. HATCN is used as a hole injection layer. The large energy shift of the highest occupied molecular orbitals (HOMO) of TAZ and the HOMO of mCP prevents the hole transport between adjacent hole-transporting layers. In the zone of exciton generation (gray color), a hole and an electron can combine due to the Coulomb forces with the excitons formation.

The correct orientation of the molecule can increase the efficiency of the doped OLEDs. The emitter with the horizontal dipole transition moment provides a much higher output coupling efficiency than the vertically oriented dipole, due to which the EQE increases [61]. Theoretically, the EQE can be increased up to 46% for the perfect horizontal orientation of emitters without using the external output structures with Φ_{PL} = 1 and Θ = 1, where Φ_{PL} is the photoluminescence quantum yield, Θ is the percentage of horizontal dipoles among all the emitting dipoles. For example, due to the high percentage of all the emitting dipoles (Θ=92%), the combination of the host component DPEPO and TADF of the CC2TA emitter as the emitting layer, provided EQE_{max} =11±1% [62] (Fig. 9). The efficiency of the horizontal orientation of the emitters was higher (31.3%) than that of the isotropic emitters (20.6%).

TADF OLED based on aggregation-induced emission.

The non-doped OLED using bis3-[9,9-dimethyl-9,10 dihydroacridine) phenyl] sulfone (mSOAD) exhibits excellent blue electroluminescence performance with the emission maximum of 488 nm and EQE =14.0%. Besides, the turn-on voltage of this OLED is 3.1 V with the maximum output of 31.7 cd/A. The AIDF OLED based on DMAC-DPS emitter demonstrates high performance characteristics. Yang and colleagues later reported about highly efficient OLEDs using two isomers as emitters: the bis-[3-(9,9-dimethyl-9,10-dihydroacridine) phenyl] sulfone isomer (mSOAD) and the bis

compound [2-(9,9-dimethyl-9,10-dihydroacridine) phenyl] of sulfone (o-$ACSO_2$). Both of these molecules have good TADF properties with excellent solubility and AIE effect due to the large twist angles between the donor and acceptor fragments (Table 2) [63, 64].

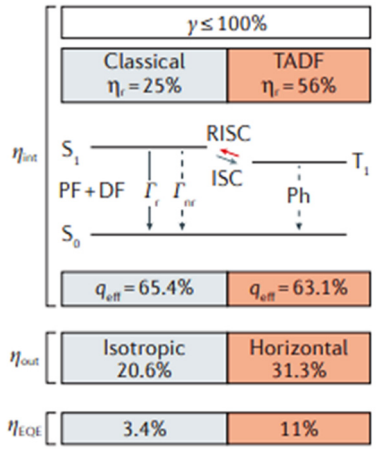

Figure 9. Individual contribution of isotropic and horizontal singlets to the external quantum efficiency (EQE or ηEQE) in the oriented EML The left column lists the typical values for the isotropic singlet emitter, and the right column lists the typical values for the oriented TADF emitter), allowing the EQE to acquire values higher than the possible ones of the classical limit. The TADF increases the percentage of the emitting excitons η_r due to the reverse conversion of the triplet excitons to the singlet state, which, in turn, increases the internal quantum efficiency (η_{int}). The horizontal orientation of the dipole transition moments in the EML increases the output efficiency (η_{out}). The radiative quantum efficiency is assumed to be the same in both scenarios. However, since the Purcell factors depend on the orientation, different values of the emission quantum efficiency ηEQE are used in the calculation

Table 2. Production performance of non-doped AIDF OLEDs

Compound	Λ_{EL} nm	V_{on} V	L_{max} cd m^{-2}	CE_{max} cd A^{-1}	PE_{max} lm W^{-1}	EQE %
m-DTPACO	480	3.9	10005	4.8	2.8	2.4
m-ACSO2	486	4.1	-	37.9	23.8	17.2
mSOAD	488	3.1	-	31.7	28.4	14.0
o-ACSO2	492	4.4	-	14.1	7.8	5.9
ECPPTT	494	5.6	10090	3.437	-	-
G2B	500[a]	4.3[a]	-	11.3	7.1	4.8
	500[b]	3.4[b]		14.0	11.5	5.7
CP-BP-DMAC	502	2.7	37680	41.6	37.9	15.0
DBT-BZ-DMAC	508	2.7	27270	43.3	35.7	14.2
G3B	513[a]	3.6[a]	-	8.7	6.6	3.6
	516[b]	2.9[b]		7.7	5.7	2.9
p-DTPACO	517	3.9	7354	10.8	8.2	3.7
ECDPTT	517	5.8	7561	2.478	-	-
DCPDAPM	521	3.2	123371	26.88	15.63	8.2
SBDBQ-DMAC	544	2.8	14578	35.4	32.7	10.1

A bit higher efficiency than that of the AIDF OLED, which is based on the DMAC-DPS emitter, is demonstrated by a light-emitting organic device, which is made using mACSO2 with electroluminescence in the blue-green region with the maximum in the region of 486 nm, the turn-on voltage of 4.1 V, the maximum current efficiency of 37.9 cd/A, with the energy efficiency of 23.8 lm/W and EQE of 17.2%. When using another isomer ɔ -ACSO2 in the OLED technology, the emission is slightly shifted to the red region of the spectrum with the maximum of 492 nm and EQE =5.9%, the OLED turn-on voltage corresponds to the value of 4.4 V with the maximum current efficiency of 14.1 cd/A and with the maximum power output of 7.8 lm/W [63]. Also, a blue-green OLED was produced by Tang and colleagues using triphenylethylene as the AIE block, the carbazole, and thianthrene-9,9,10,10-tetraoxide (ECPPTT) as the donor and acceptor, respectively [65]. The potential application of such a dye as an emitting layer in the non-doped OLED showed the maximum emission of 494 nm. The device turn-on voltage was 5.6V at the maximum brightness of 10090 cd/m^2 and with the maximum current efficiency of 3.437 cd/A. Li and colleagues [66] analyzed the application of AIE emitters, with the TADF effect inherent in them, in the non-doped green organic LEDs, which had been previously reported by Xu Zhang and colleagues [67,68]. By comparing the symmetric and asymmetric configuration of the donor and acceptor groups, i.e. using one (phenothiazine) or two different donors (phenothiazine and phenoxazine) in combination with one central acceptor component (bis-phenylsulfone), the authors concluded that the asymmetric structure of the emitters is a key condition to achieve high values of characteristics in the devices under study. Indeed, the non-doped film in the organic LEDs of the asymmetric PTSOPO provided higher current density, higher brightness, and higher EQE than of

the symmetric PTSOPT. In particular, the non-doped PTSOPO device can achieve maximum EQE= 17.0% of green electroluminescence. It should be noted, that a very low drop (0.2%) indicates to high performance of the non-doped blue-green OLED [40]. The asymmetric triple structure was also successfully investigated by Tan and colleagues [40] to obtain the organic LEDs emitting different colors. The emitter based on the D-A-D' configuration, where the D-A fragment is formed by 9-phenyl-9H-carbazole, which is bonded in the third position with the benzoyl unit (CP-BP) and uses 9,9-dimethyl-9,10. -dihydroacridine (DMAC) as the third substituent, provides the blue-green OLED generation. It takes interest that the HOMO orbitals are localized on the electron-donor part D (DMAC), and the LUMO – on the benzophenone (BP) core and they are extended to the second half of the carbazole fragment, and as a result, the emitter is characterized by a lower ΔE_{ST} value, as compared to the similar molecules containing phenoxazine (PXZ) or phenothiazine (PTZ) instead of DMAC (0.33, 0.45, and 0.11 eV for CP-BP-PXZ, CP-BP PTZ, and CP-BP-DMAC, respectively). Besides, the twisted phenyl ring in the 9th position of carbazole prevents close packing between the molecules and weakens the intermolecular interactions, thereby reducing the effect of ACQ on the film. The maximum spectral length of the emission of the OLED, based on this emitter, is 502 nm. The device is characterized by low turn on voltage (2.7 V), maximum brightness of 37,680 cd/m^2, maximum energy efficiency of 37.9 lm/W and EQE = 15.0%. It should be noted that the very low drop (0.2%) indicates to the high performance of the non-doped blue-green OLED [40].

CONCLUSIONS

The utilisation of the TADF materials as the emitters or as a host component matrix for other emitters in the OLEDs has progressed rapidly in the past few years and is considered to be the next-generation OLED technology. Nowadays, the TADF OLEDs demonstrate a high efficiency commensurate with the OLED devices based on the phosphorescent materials with organometallic complexes, which contain noble metals. The development of the molecular structures that resolve the contradiction between the large value of the emission rate constant from the excited state S_1 and the small value of ΔE_{ST} has become a notable achievement. A lot of new materials with TADF properties have also shown a promising potential for other applications in particular: in organic UV photodetectors, fluorescent sensors, and sensors based on mechanoluminochromism, which really take advantage of small ΔE_{ST} values and efficient RISC process in the TADF molecules. However, the research and development of TADF materials is still under the development stage. And so, there is a need for the development of novel molecular design strategies and detailed theoretical approaches for the development of materials on the TADF effect, which inherent some other photophysical properties. Some new conceptual solutions of the model providing the utilization and control of excitons by the TADF process should appear to expand the TADF-type materials to some other research areas.

ORCID

Serhii Melnykov, https://orcid.org/0000-0002-1093-9869; **Igor Helzhynskyy,** https://orcid.org/0000-0001-5397-4595
Pavlo Stakhira, https://orcid.org/0000-0001-5210-415X; **Tetiana Bulavinets,** https://orcid.org/0000-0001-6898-3363

REFERENCES

[1] S.R. Forrest, D.D.C. Bradley, and M.E. Thompson, Advanced Materials, **15**(13), 1043 (2003). https://doi.org/10.1002/adma.200302151
[2] Fröbel, M.; Schwab, T.; Kliem, M.; Hofmann, S.; Leo, K.; Gather, M. C. Light: Sci. Appl. **4**, e247 (2015). https://doi.org/10.1038/lsa.2015.20
[3] N. Ohon, T. Bulavinets, I. Yaremchuk, and R. Lesyuk, East European Journal of Physics, 4, 6-22 (2022). https://doi.org/10.26565/2312-4334-2022-4-01
[4] F. Dumur, Org. Electron. **21**, 27 (2015). https://doi.org/10.1016/j.orgel.2015.02.026
[5] M.A. Baldo, D.F. O'Brien, M.E. Thompson, and S.R. Forrest, Physical Review B, **60**(20), 14422 (1999). https://doi.org/10.1103/PhysRevB.60.14422
[6] M.A. Baldo, D.F. O'Brien, Y. You, A. Shoustikov, S. Sibley, M.E. Thompson, and S.R. Forrest, Nature, **395**, 151 (1998). https://doi.org/10.1038/25954
[7] H. Uoyama, K. Goushi, K. Shizu, H. Nomura, and C. Adachi, Nature, **492**, 234 (2012). https://doi.org/10.1038/nature11687
[8] Y. Tao, C. Yang, J. Qin, Chem. Soc. Rev. **40**, 2943 (2011). https://doi.org/10.1039/c0cs00160k
[9] M. Godumala, S. Choi, M.J. Cho, and D.H.J. Choi, Mater. Chem. C, **4**, 11355 (2016). https://doi.org/10.1039/C6TC04377A
[10] H. Yersin, A.F. Rausch, R. Czerwieniec, T. Hofbeck, and T. Fischer, Coordination Chemistry Reviews, **255**(21), 2622 (2011). https://doi.org/10.1016/j.ccr.2011.01.042
[11] M.Y. Wong, and E. Zysman-Colman, Adv. Mater. **29**, 1605444 (2017). https://doi.org/10.1002/adma.201605444
[12] Y. Li, J.-Y. Liu, Y.-D. Zhao, and Y.-C. Cao, Mater. Today, **20**, 258 (2017). https://doi.org/10.1016/j.mattod.2016.12.003
[13] Z. Yang, Z. Mao, Z. Xie, Y. Zhang, S. Liu, J. Zhao, J. Xu, et al., Chem. Soc. Rev. **46**, 915 (2017). https://doi.org/10.1039/C6CS00368K
[14] X. Tan, D. Volyniuk, T. Matulaitis, J. Keruckas, K. Ivaniuk, I. Helzhynskyy, P. Stakhira, and J.V.s Grazulevicius, Dyes and Pigments, **177**, 108259 (2020). https://doi.org/10.1016/j.dyepig.2020.108259
[15] A. Bucinskas, K. Ivaniuk, G. Baryshnikov, O. Bezvikonnyi, P. Stakhira, D. Volyniuk, B. Minaev, et al., Organic Electronics, **86**, 105894 (2020). https://doi.org/10.1016/j.orgel.2020.105894
[16] N. Bunzmann, B. Krugmann, S. Weissenseel, L. Kudriashova, K. Ivaniuk, and P. Stakhira, Advanced Electronic Materials, **7**, 2000702 (2021). https://doi.org/doi.org/10.1002/aelm.202000702
[17] H. Uoyama, K. Goushi, K. Shizu, H. Nomura, and C. Adachi, Nature, **492**, 234 (2012). https://doi.org/10.1038/nature11687

[18] Q.S. Zhang, B. Li, S.P. Huang, H. Nomura, H. Tanaka, and C. Adachi, Nat. Photonics, **8**, 326 (2014). https://doi.org/10.1038/nphoton.2014.12
[19] S.Y. Lee, T. Yasuda, Y.S. Yang, Q. Zhang, and C. Adachi, Angew. Chem., Int. Ed. **126**, 6520 (2014). https://doi.org/10.1002/ange.201402992
[20] J. Miller, Phys. Today, **66**, 10 (2013). https://doi.org/10.1063/PT.3.2166
[21] Y. Tao, K. Yuan, T. Chen, P. Xu, H. Li, R. Chen, C. Zheng, et al., Adv. Mater. **26**, 7931 (2014). https://doi.org/10.1002/adma.201402532
[22] D.R. Lee, B.S. Kim, C.W. Lee, Y. Im, K.S. Yook, S.H. Hwang, and J.Y. Lee, ACS Appl. Mater. Interfaces, **7**, 9625 (2015). https://doi.org/10.1021/acsami.5b01220
[23] J.W. Sun, J.H. Lee, C.K. Moon, K.H. Kim, H. Shin, and J.J. Kim, Adv. Mater. **26**, 5684 (2014). https://doi.org/10.1039/C9RA02875G
[24] Y. Im, M. Kim, Y.J. Cho, J.-A. Seo, K.S. Yook, and J.Y. Lee, Chem. Mater. **29**, 1946 (2017). https://doi.org/10.1021/acs.chemmater.6b05324
[25] L. Yao, B. Yang, and Y. Ma, Science China Chemistry, **57**, 335 (2014). https://doi.org/10.1007/s11426-013-5046-y
[26] Y. Im, S.Y. Byun, J.H. Kim, D.R. Lee, C.S. Oh, K.S. Yook, J.Y. Lee, Adv. Funct. Mater. **27**, 1603007 (2017). https://doi.org/10.1002/adfm.201603007
[27] X. Cai, Z. Qiao, M. Li, X. Wu, Y. He, X. Jiang, Y. Cao, and S.J. Su, Angew. Chem. Int. Ed. **58**, 13522 (2019). https://doi.org/10.1002/anie.201906371
[28] Z. Mao, Z. Yang, C. Xu, Z. Xie, L. Jiang, F.L. Gu, J. Zhao, et al., Chem. Sci. **10**, 7352 (2019). https://doi.org/10.1039/C9SC02282A
[29] H. Fu, Y.-M. Cheng, P.-T. Chou, and Y. Chi, Mater. Today, **14**, 472 (2011). https://doi.org/10.1016/S1369-7021(11)70211-5
[30] B. Li, Z. Yang, W. Gong, X. Chen, D.W. Bruce, S. Wang, H. Ma, et al., Adv. Opt. Mater. **9**, (2021). https://doi.org/10.1002/anie.202301896
[31] W.-C. Chen, C.-S. Lee, and Q.-X. Tong, J. Mater. Chem. C, **3**, 10957 (2015). https://doi.org/10.1039/C5TC02420J
[32] M. Zhu, and C. Yang, Chem. Soc. Rev. **42**, 4963 (2013). https://doi.org/10.1039/c3cs35440g
[33] S. Winter, S. Reineke, K. Walzer, and K. Leo, Proc. SPIE, **6999**, 69992N (2008). https://doi.org/10.1117/12.782784
[34] M. Liu, R. Komatsu, X. Cai, H. Sasabe, T. Kamata, K. Nakao, K. Liu, et al., Adv. Opt. Mater. **5**, (2017). https://doi.org/10.1002/adom.201700334
[35] W.L. Tsai, et al. Chem. Commun. **51**, 13662 (2015). https://doi.org/10.1039/C5CC05022G
[36] F.B. Dias, K.N. Bourdakos, V. Jankus, K.C. Moss, K.T. Kamtekar, V. Bhalla, J. Santos, et al., Adv. Mater. **25**, 3707 (2013). https://doi.org/10.1002/adma.201300753
[37] S. Hirata, Y. Sakai, K. Masui, H. Tanaka, S.Y. Lee, H. Nomura, N. Nakamura, et al., Nature Materials, **14**, 330 (2015). https://doi.org/10.1038/nmat4154
[38] Q. Zhang, et al., Adv. Mater. **27**, 2096 (2015). https://doi.org/10.1002/adma.201405474
[39] J. Guo, et al., Adv. Funct. Mater. **27**, 1606458 (2017). https://doi.org/10.1002/adfm.201606458
[40] J. Huang, et al., Angew. Chem. Int. Ed. **129**, 13151 (2017). https://doi.org/10.1002/anie.201706752
[41] X. Hu, N. Aizawa, M. Kim, M. Huang, Z. Li, G. Liu, H. Gao, et al., Chemical Engineering Journal, **434**, 134728, (2022). https://doi.org/10.1016/j.cej.2022.134728
[42] S. Kesari, B.K. Mishra, and A.N. Panda, Chemical Physics Letters, **791**, 139383 (2022). https://doi.org/10.1016/j.cplett.2022.139383
[43] F.B. Dias, T.J. Penfold, and A. P. Monkman, Methods Appl Fluoresc. **5**, 012001 (2017). https://doi.org/10.1088/2050-6120/aa537e
[44] S.-C. Ji, T. Zhao, Z. Wei, L. Meng, X.-D. Tao, M. Yang, X.-L. Chen, and C.-Z. Lu, Chemical Engineering Journal, **435**, 134868 (2022). https://doi.org/10.1016/j.cej.2022.134868
[45] K. Suzuki, S. Kubo, K. Shizu, T. Fukushima, A. Wakamiya, Y. Murata, C. Adachi, and H. Kaji, Angew. Chem. Int. Ed. 54, 15231 (2015). https://doi.org/10.1002/anie.201508270
[46] M.-S. Lin, et al. Mater. Chem. **22**, 16114 (2012). https://doi.org/10.1039/C2JM32717A
[47] Q. Zhang, et al. Nat. Photon. **8**, 326 (2014). https://doi.org/10.1038/nphoton.2014.12
[48] I.S. Park, S.Y. Lee, C. Adachi, and T. Yasuda, Adv. Funct. Mater. **26**, 1813 (2016). https://doi.org/10.1002/adfm.201505106
[49] Y.J. Cho, K.S. Yook, and J.Y. Lee, Adv. Mater. **26**, 6642 (2014). https://doi.org/10.1002/adma.201402188
[50] S. Hirata, et al., Nat. Mater. **14**, 330 (2015). https://doi.org/10.1038/nmat4154
[51] A. Senes, et al., J. Mater. Chem. C, **5**, 6555 (2017). https://doi.org/10.1039/C7TC01568B
[52] B.S. Kim, and J.Y. Lee, ACS Appl. Mater. Interfaces, **6**, 8396 (2014). https://doi.org/10.1021/am501301g
[53] Y. Seino, S. Inomata, H. Sasabe, Y.J. Pu, and J. Kido, Adv. Mater. **28**, 2638 (2016). https://doi.org/10.1002/adma.201503782
[54] M.P. Gaj, C. Fuentes-Hernandez, Y. Zhang, S.R. Marder, and B. Kippelen, Org. Electron. **16**, 109 (2015). https://doi.org/10.1007/s00894-016-3047-4
[55] J. Zhang, et al., Adv. Mater. **28**, 479 (2016). https://doi.org/10.1002/adma.201502772
[56] P. Dos Santos, et al., J. Phys. Chem. Lett. **7**, 3341 (2016). https://doi.org/10.1021/acs.jpclett.6b01542
[57] J. Nishide, H. Nakanotani, Y. Hiraga, and C. Adachi, Appl. Phys. Lett. **104**, 233304 (2014). https://doi.org/10.1063/1.4882456
[58] D. Zhang, L. Duan, Y. Li, D. Zhang, and Y. Qiu, J. Mater. Chem. C, **2**, 8191 (2014). https://doi.org/10.1039/C4TC01289E
[59] X.L. Li, et al., Adv. Mater. **28**, 4614 (2016). https://doi.org/10.1002/adma.201505963
[60] E. Angioni, M. Chapran, K. Ivaniuk, N. Kostiv, V. Cherpak, P. Stakhira, A. Lazauskas, et al., J. Mater. Chem. C, **4**, 3851 (2016). https://doi.org/10.1039/C6TC00750C
[61] S. Nowy, B.C. Krummacher, J. Frischeisen, N.A. Reinke, and W. Brütting, J. Appl. Phys. **104**, 123109 (2008). https://doi.org/10.1063/1.3043800
[62] C. Mayr, et al., Adv. Funct. Mater. **24**, 5232 (2014). https://doi.org/10.1002/adfm.201400495
[63] J. Li, R. Zhang, Z. Wang, B. Zhao, J. Xie, F. Zhang, H. Wang, and K. Guo, Adv. Opt. Mater. **6**(6), 1701256 (2018). https://doi.org/10.1002/adom.201701256
[64] K. Wu, Z. Wang, L. Zhan, C. Zhong, S. Gong, G. Xie, and C. Yang, J. Phys. Chem. Lett. **9**, 1547 (2018). https://doi.org/10.1021/acs.jpclett.8b00344

[65] X. Dong, S. Wang, C. Gui, H. Shi, F. Cheng, and B. Z. Tang, Tetrahedron, **74**, 497 (2018). https://doi.org/10.1016/j.tet.2017.12.022
[66] I.H. Lee, W. Song, and J.Y. Lee, Org. Electron. **29**, 22 (2016). https://doi.org/10.1002/adma.201605444
[67] S. Xu, T. Liu, Y. Mu, Y.-F. Wang, Z. Chi, C.-C. Lo, S. Liu, et al., Angew. Chem. Int. Ed. **54**, 874 (2015). https://doi.org/10.1002/anie.201409767
[68] Z. Xie, C. Chen, S. Xu, J. Li, Y. Zhang, S. Liu, J. Xu, and Z. Chi, Angew. Chem. Int. Ed. **54**, 7181 (2015). https://doi.org/10.1002/anie.201502180

ТЕРМІЧНО АКТИВОВАНА УПОВІЛЬНЕНА ФЛУОРЕСЦЕНЦІЯ В ОРГАНІЧНИХ НАПІВПРОВІДНИКАХ ТА ЇЇ ЗАСТОСУВАННЯ У СВІТЛОВИПРОМІНЮЮЧИХ ДІОДАХ

Сергій Мельников, Ігор Гельжинський, Тетяна Булавінець, Павло Стахіра
Національний університет «Львівська політехніка», кафедра електронної інженерії, пл. Св. Юра 1, Львів, Україна

Наявність ефекту термічно активованої уповільненої флуоресценції (TADF) в органічних світловипромінюючих матеріалах (емітерах), що проявляється в «збирані» триплетних екситонів в органічних напівпровідникових комплексах, які не містять благородних металів, створює чудові передумови до застосування TADF матеріалів у технології виготовлення органічних світловипромінюючих діодів (OLED). Значущий прогрес у вирішенні теоретичних та технічних завдань, що досягається в процесі розроблення високоефективних TADF матеріалів, прокладає шлях до формування майбутнього органічної електроніки. У даному огляді розглянута природа механізму генерації довготривалої флуоресценції на молекулярному рівні та сучасні стратегії проектування TADF донорно-акцепторних матеріалів, а також ексиплексних міжмолекулярних комплексів. Особлива увага акцентується на аналізі TADF емітерних амбіполярних матеріалів з сильно закрученою, жорсткою молекулярною структурою, які виявляють тенденцію до багатоканальних механізмів випромінювання та їхньої імплементації в різноманітну архітектуру OLED структур.

Ключові слова: *органічні світловипромінюючі діоди; термічно активована уповільнена флуоресценція; емітер; багатошарова структура; екситон; синглет-триплетне енергетичне розщеплення*